FISFVIFR

Contents lists available at ScienceDirect

Mechanical Systems and Signal Processing





Full length article

Time-dependent structural reliability analysis: A single-loop approximate Bayesian active learning quadrature approach

Chao Dang a[®], Pei-Pei Li a[®], Marcos A. Valdebenito a[®], Matthias G.R. Faes a,b[®]

- ^a Chair for Reliability Engineering, TU Dortmund University, Leonhard-Euler-Straße 5, Dortmund 44227, Germany
- b International Joint Research Center for Engineering Reliability and Stochastic Mechanics, Tongji University, Shanghai 200092, China

ARTICLE INFO

Communicated by M. Beer

Keywords:
Time-dependent reliability analysis
Bayesian active learning
Gaussian process regression
Stopping criterion
Learning function

ABSTRACT

Time-dependent reliability analysis allows for assessing the performance and safety of an engineering structure over its entire lifespan, accounting for inherent randomness and timevarying factors in both structural properties and external loads. However, incorporating the time dimension dramatically increases the computational complexity. To address this challenge, we propose a novel method for computationally expensive time-dependent reliability analysis, which is called 'single-loop approximate Bayesian active learning quadrature' (SL-ABALQ). First of all, estimation of the time-dependent failure probability is treated as a Bayesian inference problem with the help of Gaussian process regression. To avoid the intractability of exact Bayesian inference, an approximate Bayesian inference approach is instead developed. In this context, the mean of an approximate posterior failure probability is given, which can serve as a failure probability estimator. Moreover, we also derive an upper bound on the mean absolute deviation of the approximate posterior failure probability, which provides a measure of uncertainty for the failure probability estimator. Second, leveraging the estimator and its associated uncertainty measure, a novel stopping criterion is proposed to determine when the iterative learning process should terminate. Third, two new learning functions are introduced to identity the next best time instant and the sample point given the time instant. The performance of the proposed method is demonstrated by five numerical examples, with comparison to several existing methods. It is shown that our method can reduce the number of performance function evaluations without compromising accuracy.

1. Introduction

Ensuring the performance and safety of civil infrastructure throughout its entire service life remains a central challenge in structural engineering. Structural reliability analysis has therefore emerged as a critical tool for quantifying the probability that an engineered structure will fulfill its intended function without failure for a specified time period, explicitly accounting for various uncertainties in material properties, environmental loads, and other influential factors. Many traditional reliability analysis methods simplify the problem by assuming that the behavior of the system under consideration does not evolve with time. However, such an assumption is rarely justified because both external loads and structural properties (due to, e.g., aging, damage, wear, fatigue and corrosion) are inherently time-dependent. This time dependence can significantly affect the performance and safety of civil infrastructure. Therefore, time-dependent reliability analysis methods have also been developed, allowing the probability of failure to be assessed over the entire lifespan of a structure. Despite that, the inclusion of the time dimension significantly increases the

E-mail address: chao.dang@tu-dortmund.de (C. Dang).

^{*} Corresponding author.

computational complexity. In response to this challenge, there are roughly three main groups of methods available: analytical methods, stochastic simulation methods and surrogate modeling methods.

Analytical methods address the time-dependent reliability problem by deriving explicit (or semi-explicit) mathematical expressions for the failure probability as a function of time. One common family of analytical approaches is the out-crossing rate methods, which relate the time-dependent failure probability to the rate at which the performance function crosses from the safe domain into the failure domain. This idea traces back to Rice's seminal work [1], which introduced what is now known as Rice formula for the crossing rate of a stochastic process across a fixed threshold — later extended to the out-crossing rate concept in reliability analysis. However, analytical solutions to the Rice formula are available only for some special classes of stochastic processes, e.g., stationary Gaussian processes [2], non-stationary Gaussian processes [3] and non-stationary Lognormal processes [4]. To broaden the applicability, some other out-crossing rate methods have been developed, such as PHI2 [5], PHI2+ [6], moment-based PHI2 (MPHI2) [7] and first order time-variant reliability expansion [8]. Overall, analytical methods can provide valuable insight into the problem at hand and avoid brute-force simulations. However, they rely on simplifying assumptions (e.g., Poisson assumption) that may not always be fully justified in practical applications, and closed-form solutions are typically available only for special cases.

Instead of pursing explicit (or semi-explicit) formulas, stochastic simulation methods estimate the time-dependent failure probability by running many random simulations of the system's behavior over the period of interest and directly observing the failure frequency. The most representative method in this category is the plain Monte Carlo simulation (MCS). Although widely applicable, it requires a considerably large number of performance function evaluations for a small failure probability. This leads to the development of more efficient stochastic simulation techniques such as subset simulation (SS) [9,10], importance sampling (IS) [11–14] and line sampling [15]. Compared to analytical methods, stochastic simulation methods impose minimal assumptions about the underlying problem and offer broad versatility. However, they often demand a large number of performance function evaluations, which can render practical application computationally challenging.

Surrogate modeling methods substitute the original time-dependent performance function with a surrogate model that is computationally cheap to evaluate. Once trained, this surrogate model is typically coupled with stochastic simulation techniques to estimate the time-dependent failure probability. Examples of surrogate modeling methods are the response surface method [16], polynomial chaos expansion [17] and support vector machine [18]. Notably, active learning Kriging (AK) and Gaussian process regression (GPR) methods have received considerable attention for addressing time-dependent reliability problems. In this context, existing developments typically follow one of the two schemes: double-loop scheme and single-loop scheme. The double-loop scheme is essentially an extreme response surrogate approach: an active-learning Kriging model is built in the outer loop to approximate the performance function's extreme response over the time interval, while a separate Kriging model in the inner loop identifies the extreme response for each sample trajectory. This class includes the nested extreme response surface approach [19], mixed efficient global optimization (EGO) method [20], parallel EGO method [21], AK coupled with IS (AK-co-IS) and AK coupled with SS (AK-co-SS) [22] and IS-based double-loop Kriging [23]. On the contrary, the single-loop approach constructs a global response surrogate model for the underlying time-dependent performance function. A non-exhaustive list of such methods comprises the single-loop Kriging (SILK) method [24], single-loop adaptive sampling method [25], active failure-pursuing Kriging (AFPK) method [26], realtime estimation error-guided sampling (REAL) method [27], single-loop Kriging method considering the first failure instant [28], single-loop Kriging coupled with SS (SLK-co-SS) method [29], estimation variance reduction-guided adaptive Kriging method (VARAK) method [30], subdomain uncertainty-guided Kriging (SUK) method [31], single-loop GPR based-active learning (SL-GPR-AL) method [32] and error-informed parallel adaptive Kriging (EPAK) method [33]. In general, surrogate modeling methods can leverage the strengths of both worlds, i.e., fast evaluations from surrogates and robust probability estimation from simulation. Recent studies have shown that single-loop active learning methods can achieve a commendable balance between computational efficiency and predictive accuracy in time-dependent reliability analysis. Nevertheless, owing to factors such as improper stopping criteria and learning functions, existing single-loop methods may still suffer from slow or unreliable convergence behavior, low sampling efficiency, and limited robustness.

The first author and his co-workers have recently advanced time-independent reliability analysis from a distinct perspective by superimposing active learning atop Bayesian inference, yielding several high-performing Bayesian active learning methods (e.g., [34–38]). This conceptual idea is also helpful for addressing time-dependent reliability problems, as illustrated by two preliminary studies [39,40]. Despite these promising results, the full potential has been largely unexplored. To this end, the main objective of this paper is to develop a novel method for computationally expensive time-dependent reliability analysis by exploring both the single-loop formulation and Bayesian active learning concept. The resulting method is called 'single-loop approximate Bayesian active learning quadrature' (SL-ABALQ). The main contributions of this study can be summarized as follows. First, by leveraging the Bayesian nature of GPR, we develop an approximate Bayesian inference scheme for the time-dependent failure probability, yielding both a failure probability estimator and its associated uncertainty measure. This approach essentially helps to avoid the potential intractability of exact Bayesian inference. Second, a principled stopping criterion is proposed to determinate when the iterative learning process should terminate. Third, two learning functions are introduced to identify the next best time instant and the sample point of random variables and stochastic processes (at the identified time instant) at which to evaluate the true performance function in case the stopping criterion is not satisfied.

The remainder of this paper is organized as follows. Section 2 provides background on time-dependent structural reliability analysis. The proposed SL-ABALQ method is introduced in Section 3. Five numerical examples are studied in Section 4 to validate the performance of the proposed method. Finally, Section 5 summarizes and concludes the present study, and also highlights future research.

2. Time-dependent structural reliability analysis

This section provides some preliminary knowledge on time-dependent structural reliability analysis. Section 2.1 gives the mathematical definition of the time-dependent failure probability. Section 2.2 outlines the discretization of stochastic processes. Section 2.3 then introduces how the time-dependent failure probability is estimated by using the plain MCS.

2.1. Definition of the time-dependent failure probability

Without loss of generality, let us consider a time-dependent performance function of the form:

$$g(X(\omega_X), Y(\omega_Y, t), t) : \mathbb{R}^{d_1} \times \mathbb{R}^{d_2} \times \mathbb{R} \to \mathbb{R},$$
 (1)

where $X(\omega_X) = [X_1(\omega_X), X_2(\omega_X), \dots, X_{d_1}(\omega_X)] \in D_X \subseteq \mathbb{R}^{d_1}$ is a vector of d_1 continuous random variables with support D_X , $Y(\omega_Y, t) = [Y_1(\omega_Y, t), Y_2(\omega_Y, t), \dots, Y_{d_2}(\omega_Y, t)] \in D_Y \subseteq \mathbb{R}^{d_2}$ is a vector of d_2 continuous-time stochastic processes with support D_Y ; $\omega_X \in \Omega_X$ and $\omega_Y \in \Omega_Y$ denote two outcomes in the sample spaces Ω_X and Ω_Y , respectively; and $t \in \mathbb{R}$ represents time parameter, which is constrained to a specific interval $[t_0, t_f]$. In the sequel, the symbols ω_X and ω_Y are omitted when there is no risk of confusion. The stochastic processes involved are assumed to be second-order (i.e., square-integrable). By convention, failure occurs when the time-dependent performance function takes a negative value at any time within $[t_0, t_f]$. The time-dependent failure probability is formally defined by:

$$P_{f}(t_{0}, t_{f}) = \mathbb{P}\left\{g(X, Y(t), t) < 0, \exists t \in [t_{0}, t_{f}]\right\},\tag{2}$$

where \mathbb{P} is the probability operator. Equivalently, by appealing to the minimum value of the performance function over time, it can also be expressed as:

$$P_{f}(t_{0}, t_{f}) = \mathbb{P}\left\{\min_{t \in [t_{0}, t_{f}]} g(\boldsymbol{X}, \boldsymbol{Y}(t), t) < 0\right\}$$

$$= \int_{\mathcal{D}_{\boldsymbol{X}}} \int_{\Omega_{\boldsymbol{Y}}} I\left(\min_{t \in [t_{0}, t_{f}]} g(\boldsymbol{x}, \boldsymbol{y}(\omega_{\boldsymbol{Y}}, t), t) < 0\right) f_{\boldsymbol{X}}(\boldsymbol{x}) d\boldsymbol{x} d\mathbb{P}\left(\omega_{\boldsymbol{Y}}\right),$$
(3)

where I is the indicator function: it returns one if its argument is true, zero otherwise; $f_X(x)$ is the joint probability density function of X. The corresponding time-dependent reliability $R(t_0, t_f)$ is mathematically complementary to the failure probability $P_f(t_0, t_f)$, i.e., $R(t_0, t_f) = 1 - P_f(t_0, t_f)$. The indicator function will be interchangeably denoted as $I(x, \omega_Y)$, emphasizing its dependence on x (or equivalently ω_X) and ω_Y .

For most practical time-dependent reliability problems, it is unlikely that a closed-form solution for the time-dependent failure probability can be derived. Therefore, analytical approximations or numerical methods are often necessary.

2.2. Discretization of stochastic processes

The continuous-time stochastic processes Y(t) are inherently infinite-dimensional, rendering direct computation intractable. To enable numerical analysis, these processes are discretized into a finite-dimensional representation. A common approach is the Karhunen–Loève (KL) expansion (see, e.g., [41]), which decomposes a second-order stochastic process Y(t) into a finite series expansion. Denote the mean and covariance functions of Y(t) as $\mu_Y(t)$ and $c_Y(t_1,t_2)$, respectively. The KL expansion of Y(t) can then be expressed as:

$$Y(t) \approx \hat{Y}(t) = \mu_Y(t) + \sum_{i=1}^{q} \sqrt{\lambda_i} \xi_i \phi_i(t), \tag{4}$$

where $\{\lambda_i\}_{i=1}^q$ are q dominant eigenvalues of the covariance matrix C_Y , arranged in a descending order; $\{\phi_i(t)\}_{i=1}^q$ are corresponding eigenfunctions; $\{\xi_i\}_{i=1}^q$ are q uncorrelated random variables; q is the number of truncation terms, which can be specified by the explained variance ratio:

$$q = \underset{q \in [1,2,\dots,\infty]}{\arg\min} \left\{ \frac{\sum_{i=1}^{q} \lambda_i}{\sum_{i=1}^{\infty} \lambda_i} \ge \eta \right\},\tag{5}$$

where η is a user-defined threshold. In this study, the time interval of interest $[t_0, t_f]$ is discretized into n_t equally spaced time points, $t_0, t_1, \ldots, t_{n_t-2}, t_{n_t-1} = t_f$, where the time step is given by $\Delta t = (t_f - t_0)/(n_t - 1)$.

2.3. Time-dependent failure probability analysis by MCS

To estimate the time-dependent failure probability $P_f(t_0, t_f)$, the plain MCS can be employed straightforwardly. Its estimator can be formulated as:

$$\hat{P}_f(t_0, t_f) = \frac{1}{N} \sum_{i=1}^N I(\min_{i=0}^{n_f - 1} g(\mathbf{x}^{(j)}, \hat{\mathbf{y}}^{(j)}(t_i), t_i) < 0), \tag{6}$$

where $\left\{\mathbf{x}^{(j)}\right\}_{j=1}^{N}$ is a set of N random samples of X; $\left\{\hat{\mathbf{y}}^{(j)}(t_i)\right\}_{j=1}^{N}$ is a set of N random samples of $\hat{\mathbf{Y}}(t_i)$ at given time instant t_i . The coefficient of variation (CoV) of the estimator is given by:

$$CoV\left[\hat{P}_{f}(t_{0}, t_{f})\right] = \sqrt{\frac{1 - \hat{P}_{f}(t_{0}, t_{f})}{(N - 1)\hat{P}_{f}(t_{0}, t_{f})}}.$$
(7)

Indeed, the plain MCS represents a typical frequentist approach to evaluating the time-dependent failure probability integral, as defined in Eq. (3). While conceptually straightforward, the plain MCS is often not computationally feasible in practice due to the following reasons: (1) it requires $N \times n_t$ evaluations of the performance function g, where N must be large enough to ensure convergence and n_t must be large enough to mitigate errors due to time discretization; and (2) each evaluation of g may be computationally intensive (e.g., high-fidelity finite element analysis or multi-physics modeling), particularly for complex, large-scale engineering systems.

3. Proposed SL-ABALQ method

In this section, we introduce the proposed SL-ABALQ method for time-dependent structural reliability analysis. Section 3.1 gives an approximate Bayesian inference framework for the time-dependent failure probability based on the GPR. It is followed by the stopping criterion and learning functions in Sections 3.2 and 3.3, respectively. Finally, the procedure for implementing the proposed method is summarized in Section 3.4.

3.1. Approximate Bayesian inference about the time-dependent failure probability

In contrast to the frequentist approach, we seek to interpret the task of estimating the time-dependent failure probability integral (Eq. (3)) as a Bayesian inference problem. To circumvent the potential intractability of exact Bayesian inference, we pursue an approximate solution in this work. The core idea of the Bayesian interpretation is to treat the performance function g as a random function, even though it is deterministic by definition. This is motivated by the fact that the value of g at a given location $u = [x, \hat{y}(t), t]$ remains numerically unknown until it is evaluated, which is often the case in practice.

To begin, we place a Gaussian process (GP) prior over the performance function g:

$$g_0(\mathbf{u}) \sim \mathcal{GP}(m_{g_0}(\mathbf{u}), k_{g_0}(\mathbf{u}, \mathbf{u}')),$$
 (8)

where g_0 represents the prior distribution of g before any evaluations are performed; $u' = [x', \hat{y}'(t'), t']$ is another point in the input space; $m_{g_0}(u)$ and $k_{g_0}(u, u')$ are the prior mean and covariance functions, respectively.

Suppose that we have collected n input–output pairs of g, denoted as $\mathcal{D} = \{\mathcal{U}, \mathcal{Z}\}$, where $\mathcal{U} = \{u^{(i)}\}_{i=1}^n$ and $\mathcal{Z} = \{z^{(i)}\}_{i=1}^n$ with $z^{(i)} = g(u^{(i)})$. This collection is referred to as the design of computer experiments. Conditioning the GP prior on the data \mathcal{D} gives rise to the posterior distribution of g, which also follows a GP:

$$g_n(\mathbf{u}) \sim \mathcal{GP}(m_{g_n}(\mathbf{u}), k_{g_n}(\mathbf{u}, \mathbf{u}')),$$
 (9)

where g_n represents the posterior distribution of g after n observations are available; $m_{g_n}(\boldsymbol{u})$ and $k_{g_n}(\boldsymbol{u}, \boldsymbol{u}')$ are the posterior mean and covariance functions respectively, given by:

$$m_{g_n}(u) = m_{g_0}(u) + k_{g_0}(u, \mathcal{U})^{\top} K_{g_0}^{-1}(\mathcal{U}, \mathcal{U})(\mathcal{Z} - m_{g_0}(\mathcal{U})), \tag{10}$$

$$k_{g_n}(u, u') = k_{g_0}(u, u') - k_{g_0}(u, \mathcal{U})^{\top} K_{g_0}^{-1}(\mathcal{U}, \mathcal{U}) k_{g_0}(\mathcal{U}, u'),$$
(11)

where $m_{g_0}(\mathcal{U})$ is a column mean vector with its ith element being $m_{g_0}(\mathbf{u}^{(i)})$; $k_n(\mathbf{u},\mathcal{U})$ is a column covariance vector with its ith element being $k_{g_0}(\mathbf{u},\mathbf{u}^{(i)})$; $k_{g_0}(\mathcal{U},\mathbf{u}')$ is a column covariance vector with its ith element being $k_{g_0}(\mathbf{u}^{(i)},\mathbf{u}')$; $K_{g_0}(\mathcal{U},\mathcal{U})$ is an $n \times n$ covariance matrix with entry $\left[K_{g_0}\right]_{i:i} = k_{g_0}(\mathbf{u}^{(i)},\mathbf{u}^{(j)})$. For more details on the standard GPR above, one can refer to [42].

The posterior distribution of the indicator function I can be defined as:

$$I_n(\mathbf{x}, \omega_{\mathbf{Y}}) = \begin{cases} 1, & \min_{j=0}^{n_t-1} g_n(\mathbf{x}, \hat{\mathbf{y}}(\omega_{\mathbf{Y}}, t_j), t_j) < 0, \\ 0, & \text{otherwise.}, \end{cases}$$
 (12)

where I_n represents the posterior distribution conditional on \mathcal{D} . In fact, it can be referred to as a generalized Bernoulli process (GBP) [43,44].

According to [39], the posterior mean and variance functions of the indicator function I can be given by:

$$m_{I_n}(\mathbf{x}, \omega_{\mathbf{Y}}) = 1 - \int_{s \ge \mathbf{0}} \varphi_{n_t}(s; \mathbf{m}_{g_n}, \mathbf{K}_{g_n}) \mathrm{d}s, \tag{13}$$

$$\sigma_{I_n}^2(\boldsymbol{x}, \omega_{\boldsymbol{Y}}) = \int_{s>0} \varphi_{n_t}(s; \boldsymbol{m}_{g_n}, \boldsymbol{K}_{g_n}) \mathrm{d}s \left(1 - \int_{s>0} \varphi_{n_t}(s; \boldsymbol{m}_{g_n}, \boldsymbol{K}_{g_n}) \mathrm{d}s \right), \tag{14}$$

where $\varphi_{n_t}(s; \boldsymbol{m}_{g_n}, \boldsymbol{K}_{g_n})$ is the joint PDF of n_t -variate normal distribution with mean \boldsymbol{m}_{g_n} (with its ith element being $m_{g_n}(\boldsymbol{u}|t=t_i)$) and covariance \boldsymbol{K}_{g_n} (with its (i,j)-th entry being $k_{g_n}(\boldsymbol{u}|t=t_i,\boldsymbol{u}'|t'=t_j)$). Note that the integrals involved in Eqs. (13) and (14)

are analytically intractable, so MCS is typically employed. However, this in turn will lead to difficulties in obtaining the posterior statistics of the time-dependent failure probability.

To overcome the aforementioned issue, this study proposes an approximate analytic strategy. Let us first assume that $g_n(\boldsymbol{u}|t=t_0)$, $g_n(\boldsymbol{u}|t=t_1)$, ..., $g_n(\boldsymbol{u}|t=t_{n,-1})$ are perfectly positively linearly correlated, i.e.,

$$g_n(\mathbf{x}, \hat{\mathbf{y}}(\omega_Y, t_i), t_i) = m_{\varepsilon_n}(\mathbf{x}, \hat{\mathbf{y}}(\omega_Y, t_i), t_i) + \sigma_{\varepsilon_n}(\mathbf{x}, \hat{\mathbf{y}}(\omega_Y, t_i), t_i)Z, \tag{15}$$

where $\sigma_{g_n}(\cdot)$ is the posterior standard deviation function of g, i.e., $\sigma_{g_n}(\cdot) = \sqrt{k_{g_n}(\cdot,\cdot)}$; Z is the standard normal variable. It is worth noting that the true correlation coefficient ρ between any two time instances is governed by the posterior covariance function (Eq. (11)), which lies within [-1,1]. While the assumption $\rho=1$ may overestimate the true correlation, it greatly simplifies the temporal dependence structure and leads to useful results, as will be shown. Under the perfect correlation assumption, we can replace the original posterior indicator function I_n with an approximate version \tilde{I}_n , which is defined as:

$$\tilde{I}_{n}(\mathbf{x}, \omega_{\mathbf{Y}}) = \begin{cases} 1, & \min_{j=0}^{n_{t}-1} m_{g_{n}}(\mathbf{x}, \hat{\mathbf{y}}(\omega_{\mathbf{Y}}, t_{j}), t_{j}) + \sigma_{g_{n}}(\mathbf{x}, \hat{\mathbf{y}}(\omega_{\mathbf{Y}}, t_{j}), t_{j}) Z < 0, \\ 0, & \text{otherwise.} \end{cases}$$

$$(16)$$

which also follows a GBP.

The mean and variance functions of \tilde{I}_n can be derived as:

$$m_{\tilde{I}_{n}}(\mathbf{x}, \omega_{\mathbf{Y}}) = \mathbb{E}\left[\tilde{I}_{n}(\mathbf{x}, \omega_{\mathbf{Y}})\right]$$

$$= \mathbb{P}\left(\tilde{I}_{n}(\mathbf{x}, \omega_{\mathbf{Y}}) = 1\right)$$

$$= \Phi\left(-\min_{i=0}^{n_{r}-1} \frac{m_{g_{n}}(\mathbf{x}, \hat{\mathbf{y}}(\omega_{\mathbf{Y}}, t_{i}), t_{i})}{\sigma_{g_{n}}(\mathbf{x}, \hat{\mathbf{y}}(\omega_{\mathbf{Y}}, t_{i}), t_{i})}\right),$$

$$(17)$$

$$\sigma_{\tilde{I}_{n}}^{2}(\mathbf{x}, \omega_{\mathbf{Y}}) = \mathbb{V}\left[\tilde{I}_{n}(\mathbf{x}, \omega_{\mathbf{Y}})\right]$$

$$= \mathbb{P}\left(\tilde{I}_{n}(\mathbf{x}, \omega_{\mathbf{Y}}) = 0\right) \times \mathbb{P}\left(\tilde{I}_{n}(\mathbf{x}, \omega_{\mathbf{Y}}) = 1\right)$$

$$= \Phi\left(-\min_{i=0}^{n_{t}-1} \frac{m_{g_{n}}(\mathbf{x}, \hat{\mathbf{y}}(\omega_{\mathbf{Y}}, t_{i}), t_{i})}{\sigma_{g_{n}}(\mathbf{x}, \hat{\mathbf{y}}(\omega_{\mathbf{Y}}, t_{i}), t_{i})}\right) \Phi\left(\min_{i=0}^{n_{t}-1} \frac{m_{g_{n}}(\mathbf{x}, \hat{\mathbf{y}}(\omega_{\mathbf{Y}}, t_{i}), t_{i})}{\sigma_{g_{n}}(\mathbf{x}, \hat{\mathbf{y}}(\omega_{\mathbf{Y}}, t_{i}), t_{i})}\right),$$
(18)

where \mathbb{E} and \mathbb{V} denote the expectation and variance operators, respectively. Note that $m_{\tilde{I}_n}(\mathbf{x},\omega_{\mathbf{Y}})$ can be regarded a smoothed version of the indicator function $I(\min_{i=0}^{n_t-1}g(\mathbf{x},\hat{\mathbf{y}}(\omega_{\mathbf{Y}},t_i),t_i)<0)$. As $\sigma_{g_n}\to 0$, the former converges to the latter. In the limiting conditions (i.e., $q\to\infty$, $n_t\to\infty$ and $\sigma_{g_n}\to 0$), $m_{\tilde{I}_n}(\mathbf{x},\omega_{\mathbf{Y}})$ can approach the true indicator function $I(\mathbf{x},\omega_{\mathbf{Y}})$.

Further, the resulting approximate posterior distribution of the time-dependent failure probability can be expressed as:

$$\tilde{P}_{f,n}(t_0, t_f) = \int_{D_{\mathbf{Y}}} \int_{\Omega_{\mathbf{Y}}} \tilde{I}_n(\mathbf{x}, \omega_{\mathbf{Y}}) f_{\mathbf{X}}(\mathbf{x}) \mathrm{d}\mathbf{x} \mathrm{d}\mathbb{P}\left(\omega_{\mathbf{Y}}\right). \tag{19}$$

Using Tonelli's theorem, the mean of $\tilde{P}_{f,n}(t_0,t_f)$ can be derived as:

$$m_{\tilde{P}_{f,n}(t_{0},t_{f})} = \mathbb{E}\left[\tilde{P}_{f,n}(t_{0},t_{f})\right]$$

$$= \mathbb{E}\left[\int_{D_{X}} \int_{\Omega_{Y}} \tilde{I}_{n}(\mathbf{x},\omega_{Y}) f_{X}(\mathbf{x}) d\mathbf{x} d\mathbb{P}\left(\omega_{Y}\right)\right]$$

$$= \int_{D_{X}} \int_{\Omega_{Y}} \mathbb{E}\left[\tilde{I}_{n}(\mathbf{x},\omega_{Y})\right] f_{X}(\mathbf{x}) d\mathbf{x} d\mathbb{P}\left(\omega_{Y}\right)$$

$$= \int_{D_{X}} \int_{\Omega_{Y}} \tilde{m}_{\hat{I}_{n}}(\mathbf{x},\omega_{Y}) f_{X}(\mathbf{x}) d\mathbf{x} d\mathbb{P}\left(\omega_{Y}\right)$$

$$= \int_{D_{X}} \int_{\Omega_{Y}} \Phi\left(-\min_{i=0}^{n_{i}-1} \frac{m_{g_{n}}(\mathbf{x},\hat{\mathbf{y}}(\omega_{Y},t_{i}),t_{i})}{\sigma_{g_{n}}(\mathbf{x},\hat{\mathbf{y}}(\omega_{Y},t_{i}),t_{i})}\right) f_{X}(\mathbf{x}) d\mathbf{x} d\mathbb{P}\left(\omega_{Y}\right).$$

$$(20)$$

Even with the perfect correlation assumption (Eq. (15)), $m_{\tilde{P}_{f,n}(l_0,t_f)}$ converges, in principle, to the true time-dependent failure probability $P_f(t_0,t_f)$ in the limiting conditions (i.e., $q\to\infty$, $n_t\to\infty$ and $\sigma_{g_n}\to 0$). This is because the integrand of $m_{\tilde{P}_{f,n}(l_0,t_f)}$, namely $m_{\tilde{I}_n}(x,\omega_Y)$, approaches the true indication function $I(x,\omega_Y)$, as discussed earlier. Therefore, $m_{\tilde{P}_{f,n}(l_0,t_f)}$ can be used as an estimator of the time-dependent failure probability $P_f(t_0,t_f)$. While this estimator has been suggested in previous studies [39,40], it is derived from a completely different perspective in this paper. The advantage of this alternative viewpoint is that it offers a clearer theoretical justification. In addition to the time-dependent failure probability estimator, a measure of the underlying uncertainty is also necessary.

To this end, we now examine the mean absolute deviation of the approximate posterior failure probability $\tilde{P}_{f,n}(t_0,t_f)$:

$$\mathbb{E}\left[\left|\tilde{P}_{f,n}(t_{0},t_{f}) - m_{\tilde{P}_{f,n}(t_{0},t_{f})}\right|\right] \\
= \mathbb{E}\left[\left|\int_{D_{X}} \int_{\Omega_{Y}} \tilde{I}_{n}(\mathbf{x},\omega_{Y}) f_{X}(\mathbf{x}) d\mathbf{x} d\mathbb{P}\left(\omega_{Y}\right) - \int_{D_{X}} \int_{\Omega_{Y}} m_{\tilde{I}_{n}}(\mathbf{x},\omega_{Y}) f_{X}(\mathbf{x}) d\mathbf{x} d\mathbb{P}\left(\omega_{Y}\right)\right|\right] \\
= \mathbb{E}\left[\left|\int_{D_{X}} \int_{\Omega_{Y}} \left[\tilde{I}_{n}(\mathbf{x},\omega_{Y}) - m_{\hat{I}_{n}}(\mathbf{x},\omega_{Y})\right] f_{X}(\mathbf{x}) d\mathbf{x} d\mathbb{P}\left(\omega_{Y}\right)\right|\right] \\
\leq \mathbb{E}\left[\int_{D_{X}} \int_{\Omega_{Y}} \left|\tilde{I}_{n}(\mathbf{x},\omega_{Y}) - m_{\hat{I}_{n}}(\mathbf{x},\omega_{Y})\right| f_{X}(\mathbf{x}) d\mathbf{x} d\mathbb{P}(\omega_{Y})\right] \\
= \int_{D_{X}} \int_{\Omega_{Y}} \mathbb{E}\left[\left|\tilde{I}_{n}(\mathbf{x},\omega_{Y}) - m_{\hat{I}_{n}}(\mathbf{x},\omega_{Y})\right|\right] f_{X}(\mathbf{x}) d\mathbf{x} d\mathbb{P}(\omega_{Y}) \\
= \int_{D_{X}} \int_{\Omega_{Y}} \left[\left|1 - m_{\hat{I}_{n}}(\mathbf{x},\omega_{Y}) \right| \times \mathbb{P}\left(\tilde{I}_{n}(\mathbf{x},\omega_{Y}) = 1\right) + \left|0 - m_{\hat{I}_{n}}(\mathbf{x},\omega_{Y})\right| \times \mathbb{P}\left(\tilde{I}_{n}(\mathbf{x},\omega_{Y}) = 0\right)\right] f_{X}(\mathbf{x}) d\mathbf{x} d\mathbb{P}(\omega_{Y}) \\
= 2 \int_{D_{X}} \int_{\Omega_{Y}} \Phi\left(-\min_{i=0}^{n_{i}-1} \frac{m_{n}(\mathbf{x},\hat{\mathbf{y}}(\omega_{Y},t_{i}),t_{i})}{\sigma_{n}(\mathbf{x},\hat{\mathbf{y}}(\omega_{Y},t_{i}),t_{i})}\right) \Phi\left(\min_{i=0}^{n_{i}-1} \frac{m_{n}(\mathbf{x},\hat{\mathbf{y}}(\omega_{Y},t_{i}),t_{i})}{\sigma_{n}(\mathbf{x},\hat{\mathbf{y}}(\omega_{Y},t_{i}),t_{i})}\right) f_{X}(\mathbf{x}) d\mathbf{x} d\mathbb{P}(\omega_{Y})$$

If we denote:

$$\pi_{n} = \int_{\mathcal{D}_{\boldsymbol{X}}} \int_{\Omega_{\boldsymbol{Y}}} \boldsymbol{\Phi} \left(-\min_{i=0}^{n_{t}-1} \frac{m_{n}(\boldsymbol{x}, \hat{\boldsymbol{y}}(\omega_{\boldsymbol{Y}}, t_{i}), t_{i})}{\sigma_{n}(\boldsymbol{x}, \hat{\boldsymbol{y}}(\omega_{\boldsymbol{Y}}, t_{i}), t_{i})} \right) \boldsymbol{\Phi} \left(\min_{i=0}^{n_{t}-1} \frac{m_{n}(\boldsymbol{x}, \hat{\boldsymbol{y}}(\omega_{\boldsymbol{Y}}, t_{i}), t_{i})}{\sigma_{n}(\boldsymbol{x}, \hat{\boldsymbol{y}}(\omega_{\boldsymbol{Y}}, t_{i}), t_{i})} \right) f_{\boldsymbol{X}}(\boldsymbol{x}) d\boldsymbol{x} d\mathbb{P}(\omega_{\boldsymbol{Y}}),$$

$$(22)$$

then Ineq. (21) can be written succinctly as:

$$\mathbb{E}\left[\left|\tilde{P}_{f,n}(t_0,t_f) - m_{\tilde{P}_{f,n}(t_0,t_f)}\right|\right] \le 2\pi_n. \tag{23}$$

This implies that when $\pi_n \to 0$, $\tilde{P}_{f,n}(t_0,t_f)$ converges in expectation to its mean $m_{\tilde{P}_{f,n}(t_0,t_f)}$. Thus, π_n naturally quantifies the uncertainty of the time-dependent failure probability estimator $m_{\tilde{P}_{f,n}(t_0,t_f)}$.

It is noted that closed-form expressions for both $m_{\tilde{p}_{f,n}(t_0,I_f)}$ and π_n' are unavailable, so in this study we approximate them numerically using MCS. The respective MCS estimators are given by:

$$\hat{m}_{\bar{P}_{f,n}(t_0,t_f)} = \frac{1}{N} \sum_{j=1}^{N} \boldsymbol{\Phi} \left(-\min_{i=0}^{n_i-1} \frac{m_{g_n}(\mathbf{x}^{(j)}, \hat{\mathbf{y}}^{(j)}(t_i), t_i)}{\sigma_{g_n}(\mathbf{x}^{(j)}, \hat{\mathbf{y}}^{(j)}(t_i), t_i)} \right), \tag{24}$$

$$\hat{\pi}_{n} = \frac{1}{N} \sum_{i=1}^{N} \boldsymbol{\Phi} \left(-\min_{i=0}^{n_{i}-1} \frac{m_{g_{n}}(\mathbf{x}^{(j)}, \hat{\mathbf{y}}^{(j)}(t_{i}), t_{i})}{\sigma_{g_{n}}(\mathbf{x}^{(j)}, \hat{\mathbf{y}}^{(j)}(t_{i}), t_{i})} \right) \boldsymbol{\Phi} \left(\min_{i=0}^{n_{i}-1} \frac{m_{g_{n}}(\mathbf{x}^{(j)}, \hat{\mathbf{y}}^{(j)}(t_{i}), t_{i})}{\sigma_{g_{n}}(\mathbf{x}^{(j)}, \hat{\mathbf{y}}^{(j)}(t_{i}), t_{i})} \right),$$
(25)

where $\left\{ m{x}^{(j)} \right\}_{j=1}^N$ is a sequence of N random samples drawn according to $f_{m{X}}(m{x})$; $\left\{ \hat{m{y}}^{(j)}(t_i) \right\}_{j=1}^N$ at a given i is a set of N random samples of $\hat{m{Y}}(t_i)$. The associated variances for $\hat{m}_{\hat{P}_{f,n}(t_0,t_f)}$ and $\hat{\pi}_n$ are :

$$\mathbb{V}\left[\hat{m}_{\bar{P}_{f,n}(t_0,t_f)}\right] = \frac{1}{N(N-1)} \sum_{j=1}^{N} \left[\boldsymbol{\Phi}\left(-\min_{i=0}^{n_t-1} \frac{m_{g_n}(\mathbf{x}^{(j)}, \hat{\mathbf{y}}^{(j)}(t_i), t_i)}{\sigma_{g_n}(\mathbf{x}^{(j)}, \hat{\mathbf{y}}^{(j)}(t_i), t_i)} \right) - \hat{m}_{\bar{P}_{f,n}(t_0,t_f)} \right]^2.$$
(26)

$$\mathbb{V}\left[\hat{\pi}_{n}\right] = \frac{1}{N(N-1)} \sum_{j=1}^{N} \left[\boldsymbol{\Phi} \left(-\min_{i=0}^{n_{t}-1} \frac{m_{g_{n}}(\mathbf{x}^{(j)}, \hat{\mathbf{y}}^{(j)}(t_{i}), t_{i})}{\sigma_{g_{n}}(\mathbf{x}^{(j)}, \hat{\mathbf{y}}^{(j)}(t_{i}), t_{i})} \right) \boldsymbol{\Phi} \left(\min_{i=0}^{n_{t}-1} \frac{m_{g_{n}}(\mathbf{x}^{(j)}, \hat{\mathbf{y}}^{(j)}(t_{i}), t_{i})}{\sigma_{g_{n}}(\mathbf{x}^{(j)}, \hat{\mathbf{y}}^{(j)}(t_{i}), t_{i})} \right) - \hat{\pi}_{n} \right]^{2}.$$

$$(27)$$

3.2. Stopping criterion

Having obtained the time-dependent failure probability estimate, a natural question is whether this estimate is sufficiently accurate. This, in turn, hinges on defining an appropriate stopping criterion. To do so, let us first study the relative mean absolute deviation of $\tilde{P}_{f,n}(t_0,t_f)$. Dividing both sides of Ineq. (23) by $m_{\tilde{P}_{f,n}(t_0,t_f)}$ (assumed nonzero), we have:

$$\mathbb{E}\left[\left|\frac{\tilde{P}_{f,n}(t_0,t_f) - m_{\tilde{P}_{f,n}(t_0,t_f)}}{m_{\tilde{P}_{f,n}(t_0,t_f)}}\right|\right] \le \frac{2\pi_n}{m_{\tilde{P}_{f,n}(t_0,t_f)}}.$$
(28)

This suggests that the relative mean absolute deviation of $\tilde{P}_{f,n}(t_0,t_f)$ is actually bounded by $2\pi_n/m_{\tilde{P}_{f,n}(t_0,t_f)}$. If π_n is small relative to $m_{\tilde{P}_{f,n}(t_0,t_f)}$, $\tilde{P}_{f,n}(t_0,t_f)$ will concentrate around its mean value $m_{\tilde{P}_{f,n}(t_0,t_f)}$.

Based on Ineq. (28), the following stopping criterion is proposed:

$$\frac{\pi_n}{m_{\tilde{P}_{f,n}(t_0,t_f)}} < \epsilon,\tag{29}$$

where ϵ is a user-specified threshold. The stopping criterion guarantees that the relative mean absolute deviation of $\tilde{P}_{f,n}(t_0,t_f)$ is at most 2ϵ . In practice, $m_{\tilde{P}_{f,n}(t_0,t_f)}$ and π_n are replaced by their estimates $\hat{m}_{\tilde{P}_{f,n}(t_0,t_f)}$ and $\hat{\pi}_n$, respectively.

3.3. Learning functions

If the stopping criterion in Ineq. (29) is not satisfied, the best next point $\left\{x^{(n+1)},\hat{y}^{(n+1)}(t^{(n+1)}),t^{(n+1)}\right\}$ where to evaluate the true performance function has to be selected, with the aim of further improving the accuracy of the time-dependent failure probability estimate. This choice is typically guided by one or more learning (or acquisition) functions, which quantify the utility of each candidate point. The next point is then identified by maximizing (or minimizing) these functions. In this study, we propose two novel learning functions: one for selecting $t^{(n+1)}$, and another for selecting $t^{(n+1)}$, $t^{(n+1)}$, $t^{(n+1)}$.

For ease of understanding, the second learning function is presented first:

$$\mathcal{L}_{n}(\mathbf{x}, \hat{\mathbf{y}}(t_{i}), t_{i}) = \underbrace{\sigma_{g_{n}}^{2}(\mathbf{x}, \hat{\mathbf{y}}(t_{i}), t_{i})}_{\text{D}} \underbrace{\Phi\left(-\frac{m_{g_{n}}(\mathbf{x}, \hat{\mathbf{y}}(t_{i}), t_{i})}{\sigma_{g_{n}}(\mathbf{x}, \hat{\mathbf{y}}(t_{i}), t_{i})}\right) \Phi\left(\frac{m_{g_{n}}(\mathbf{x}, \hat{\mathbf{y}}(t_{i}), t_{i})}{\sigma_{g_{n}}(\mathbf{x}, \hat{\mathbf{y}}(t_{i}), t_{i})}\right) f_{\mathbf{X}}(\mathbf{x}) f_{\hat{\mathbf{Y}}(t_{i})}(\hat{\mathbf{y}}(t_{i})),}_{\mathbf{Y}(t_{i})}$$

$$(30)$$

where term ② is derived from the integrand of π_n by omitting the min operation, which is multiplied by the posterior variance of g (i.e., term ①). The learning function attains large values when m_{g_n} is near zero, σ_{g_n} is high or the joint PDF is large. Besides, the larger $\mathcal{L}_n(\mathbf{x},\hat{\mathbf{y}}(t_i),t_i)$ is, the more promising the candidate point $\left\{\mathbf{x},\hat{\mathbf{y}}(t_i),t_i\right\}$ is deemed. In this regard, the proposed learning function can naturally trade off exploitation and exploration.

Then, we introduce our first learning function, which is simply the integral of \mathcal{L}_n :

$$I\mathcal{L}_n(t_i) = \int_{D_{\mathbf{X}}} \int_{D_{\mathbf{Y}}} \mathcal{L}_n(\mathbf{x}, \hat{\mathbf{y}}(t_i), t_i) d\mathbf{x} d\hat{\mathbf{y}}(t_i).$$
(31)

By integrating \mathcal{L}_n over \mathcal{D}_X and \mathcal{D}_Y , the function \mathcal{IL}_n can average out the uncertainty associated with X and $\hat{Y}(t_i)$ and provide a global measure of the learning potential of t_i . The learning function is approximated by using MCS:

$$\widehat{IL}_{n}(t_{i}) = \frac{1}{N} \sum_{j=1}^{N} \sigma_{g_{n}}^{2}(\mathbf{x}^{(j)}, \hat{\mathbf{y}}^{(j)}(t_{i}), t_{i}) \boldsymbol{\Phi} \left(- \min_{i=0}^{n_{i}-1} \frac{m_{g_{n}}(\mathbf{x}^{(j)}, \hat{\mathbf{y}}^{(j)}(t_{i}), t_{i})}{\sigma_{g_{n}}(\mathbf{x}^{(j)}, \hat{\mathbf{y}}^{(j)}(t_{i}), t_{i})} \right) \boldsymbol{\Phi} \left(\min_{i=0}^{n_{t}-1} \frac{m_{g_{n}}(\mathbf{x}^{(j)}, \hat{\mathbf{y}}^{(j)}(t_{i}), t_{i})}{\sigma_{g_{n}}(\mathbf{x}^{(j)}, \hat{\mathbf{y}}^{(j)}(t_{i}), t_{i})} \right).$$
(32)

The best next time instant $t^{(n+1)}$ is identified by maximizing $\widehat{\mathcal{IL}}_n(t_i)$:

$$t^{(n+1)} = \underset{t_i \in [t_0, t_1, \dots, t_{n_i-1}]}{\arg \max} \widehat{IL}_n(t_i).$$
(33)

The best next sample point $\left\{\mathbf{x}^{(n+1)}, \hat{\mathbf{y}}^{(n+1)}(t^{(n+1)})\right\}$ is obtained by maximizing \mathcal{L}_n conditional on $t_i = t^{(n+1)}$:

$$\left\{ \boldsymbol{x}^{(n+1)}, \hat{\boldsymbol{y}}^{(n+1)}(t^{(n+1)}) \right\} = \underset{\boldsymbol{x} \in \left\{ \boldsymbol{x}^{(j)} \right\}_{j=1}^{N}, \hat{\boldsymbol{y}}(t^{(n+1)}) \in \left\{ \hat{\boldsymbol{y}}^{(j)}(t^{(n+1)}) \right\}_{j=1}^{N}}{\arg \max} \mathcal{L}_{n}(\boldsymbol{x}, \hat{\boldsymbol{y}}(t^{(n+1)}), t^{(n+1)}). \tag{34}$$

3.4. Implementation procedure of the proposed method

The implementation procedure of the proposed SL-ABALQ method is summarized below and accompanied by a flowchart in Fig. 1.

Step 1: Discretize the time interval

Discretize the time interval $[t_0, t_f]$ into n_t equally spaced nodes $t_i = t_0 + i\Delta t$, $i = 0, 1, \dots, n_t - 1$, where $\Delta t = \frac{t_f - t_0}{n_t - 1}$.

Step 2: Construct the initial sample pool

Construct the initial sample pool $S = \left\{ x^{(j)}, \hat{y}^{(j)}(t_i), t_i \right\}_{i=0,j=1}^{n_t-1,N_0}$, where $\left\{ x^{(j)} \right\}_{j=1}^{N_0}$ is a set of N_0 random samples of X generated according to $f_X(x)$ and $\left\{ \hat{y}^{(j)}(t_i) \right\}_{j=1}^{N_0}$ is a set of N_0 random samples of Y(t) at time instant t_i generated using the KL expansion. Let $N = N_0$.

Step 3: Generate the initial design of experiments

Generate the initial design of experiments $\mathcal{D} = \{\mathcal{V}, \mathcal{Z}\}$, where $\mathcal{V} = \left\{\mathbf{x}^{(l)}, \hat{\mathbf{y}}^{(l)}(t_l), t_l\right\}_{l=1}^{n_0}$ and $\mathcal{Z} = \left\{z^{(l)}\right\}_{l=1}^{n_0}$ with $z^{(l)} = g(\mathbf{x}^{(l)}, \hat{\mathbf{y}}^{(l)}(t_l), t_l)$. Note that t_l for $l = 1, 2, \dots, n_0$ are simply taken as n_0 equally spaced points on the interval $[t_0, t_f]$. Besides, $\left\{\mathbf{x}^{(l)}\right\}_{l=1}^{n_0}$ are drawn from $f_X(\mathbf{x})$ using Hammersley sequence and $\left\{\hat{\mathbf{y}}^{(l)}(t_l)\right\}_{l=1}^{n_0}$ are generated via KL expansion in conjunction with Hammersley sequence. Let $n = n_0$.

Step 4: Build the GPR model

Build the GPR model $g_n(\mathbf{x}, \hat{\mathbf{y}}(t_i), t_i)$ of the time-dependent performance function g using the experimental design \mathcal{D} . In this study, we employ MATLAB's function *fitrgp* available in the statistics and machine learning toolbox, with a constant prior mean and a squared-exponential prior covariance. The involved hyper-parameters are tuned by the maximum likelihood estimation.

Step 5: Obtain the two terms $\hat{m}_{\tilde{P}_{f_n}(t_0,t_f)}$ and $\hat{\pi}_n$

Obtain the time-dependent failure probability estimate $\hat{m}_{\tilde{P}_{f,n}(t_0,t_f)}$ and the epistemic uncertainty measure estimate $\hat{\pi}_n$ using MCS with S.

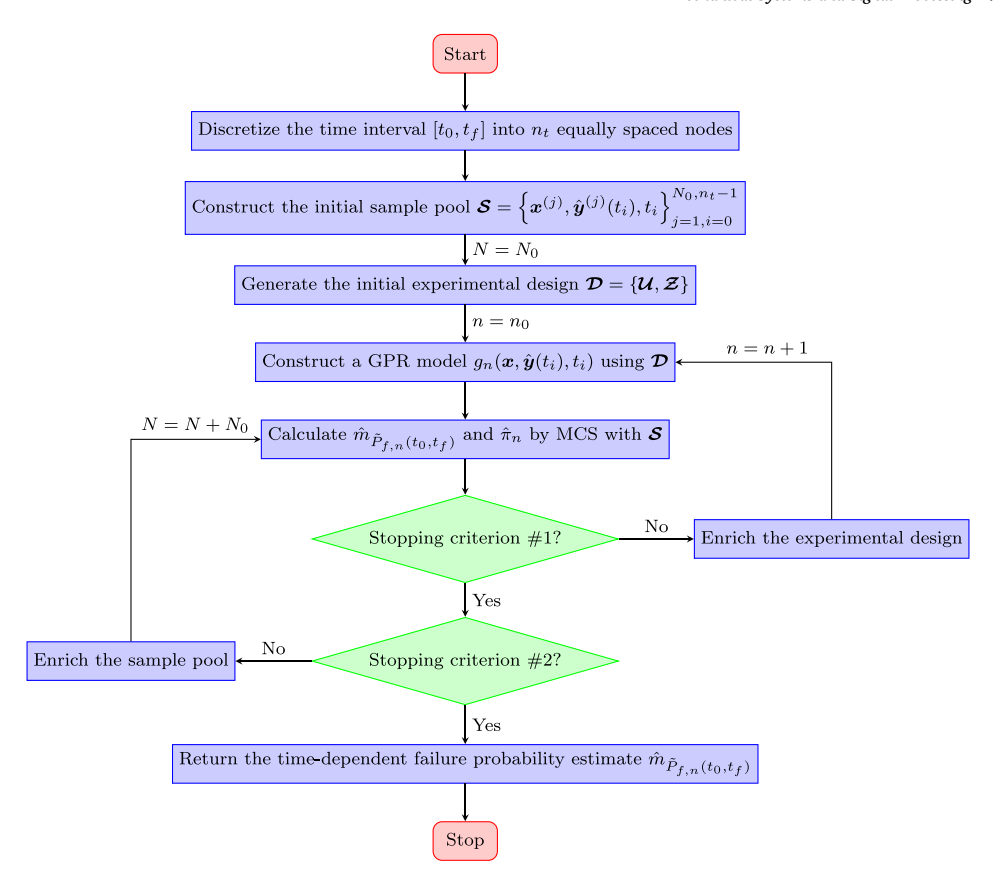


Fig. 1. Flowchart of the proposed SL-ABALQ method.

Step 6: Check the stopping criterion #1

If the stopping criterion $\frac{\hat{\pi}_n}{\hat{m}_{\tilde{P}_{f,n}(t_0,t_f)}} < \epsilon$ is met twice in a row, then proceed to **Step 8**; otherwise, go to **Step 7**.

Step 7: Enrich the design of experiments

Enrich the design of experiments \mathcal{D} with $\left\{x^{(n+1)}, \hat{y}^{(n+1)}(t^{(n+1)}), t^{(n+1)}, z^{(n+1)}\right\}$, where $t^{(n+1)}$ is obtained by Eq. (33), $\left\{x^{(n+1)}, \hat{y}^{(n+1)}(t^{(n+1)})\right\}$ is identified by Eq. (34), and $z^{(n+1)} = g(x^{(n+1)}, \hat{y}^{(n+1)}(t^{(n+1)}), t^{(n+1)})$. Let n = n+1 and go to **Step 4**.

Step 8: Check the stopping criterion #2

Calculate the CoV of the failure probability estimator $\hat{m}_{\tilde{P}_{f,n}(t_0,t_f)}$ by CoV $\left[\hat{m}_{\tilde{P}_{f,n}(t_0,t_f)}\right] = \frac{\sqrt{\mathrm{Var}\left[\hat{m}_{\tilde{P}_{f,n}(t_0,t_f)}\right]}}{\hat{m}_{\tilde{P}_{f,n}(t_0,t_f)}}$. If CoV $\left[\hat{m}_{\tilde{P}_{f,n}(t_0,t_f)}\right] < \delta$ is reached (δ is a user-defined threshold), then go to **Step 10**; otherwise, proceed to **Step 9**. It is worth noting that this stopping criterion is employed to guarantee that the size of the sample pool is adequate.

Step 9: Enrich the sample pool

Enrich the sample pool S with additional N_0 samples S^+ exactly as in Step 2. Let $N = N + N_0$ and go to Step 5.

Step 10: Return the time-dependent failure probability

Return the time-dependent failure probability estimate $\hat{m}_{\tilde{P}_{f,n}(t_0,t_f)}$ as the final result.

Remark 1. The proposed SL-ABALQ method remains applicable when the performance function takes other simpler forms, e.g., g(X,t), g(Y(t),t), g(Y(t),t), g(Y(t)).

Remark 2. Other intermediate time-dependent failure probability values $\hat{P}_f(t_0, t_i)$ for $i = 0, 1, ..., n_t - 2$ can be obtained along with $\hat{P}_f(t_0, t_f)$ as by-products. They together can provide the insight into evolution of the failure probability. However, the first $n_t - 1$ values may not be guaranteed to be as accurate as the last one.

Table 1Random variables and stochastic process of Example 1.

Symbol	Distribution	Mean	Standard deviation	Auto-correlation function
X_1	Normal	0	1	_
X_2	Normal	0	1	_
Y(t)	Gaussian process	5	1	$\exp\left(-(t_2-t_1)^2\right)$

Table 2Time-dependent failure probability results of Example 1.

Method	$N_{ m call}$		$\hat{P}_f(0,1)$	
	Mean	CoV	Mean	CoV
MCS	50×10^{7}	-	3.27×10^{-2}	0.17%
PHI2	600	_	4.22×10^{-2}	_
SILK	42.10	11.56%	3.28×10^{-2}	1.61%
REAL	40.65	9.04%	3.30×10^{-2}	5.25%
SL-GPR-AL	28.15	10.26%	3.28×10^{-2}	1.48%
Proposed SL-ABALQ	22.35	9.77%	3.24×10^{-2}	3.06%

4. Numerical examples

In order to validate the performance of the proposed SL-ABALQ method for time-dependent reliability analysis, five numerical examples are investigated in this section. Aside from n_t , the involved parameters are set as follows: $N_0 = 10^5$, $\eta = 99.5\%$, $n_0 = 10$, $\epsilon = 3\%$, $\delta = 2\%$. Several existing active learning methods (i.e., PHI2 [5], SILK [24], REAL [27] and SL-GPR-AL [32]) are also conducted in each example. The latter three methods, along with the proposed method, are each run independently 20 times, and the statistical results are reported.

4.1. Example 1: a test function

The first example considers a time-dependent performance function of the form:

$$g(X, Y(t), t) = Y(t) \exp(-t) + \exp(-\frac{X_1^2}{10}) + \frac{X_1^4}{5} - X_2 - 1,$$
(35)

where $t \in [0,1]$; X_1 and X_2 are two random variables, Y(t) is a stochastic process, as reported in Table 1. The time interval [0,1] is discretized into $n_t = 50$ equally spaced points.

Table 2 summarizes the results of six methods, i.e., MCS, PHI2, SILK, REAL, SL-GPR-AL and SL-ABALQ. The reference for the time-dependent failure probability $P_f(0,1)$ is taken as 3.27×10^{-2} (with a CoV of 0.17%), which is provided by MCS with 50×10^7 evaluations of the performance function. With 600 g-function evaluations, PHI2 yields a less accurate estimate of 4.22×10^{-2} . Among the remaining four methods, the proposed SL-ABALQ method achieves the fewest average calls to the g-function, while still yielding a mean value of the failure probability estimates that closely matches the reference and with a small CoV of 3.06%.

In addition to $\hat{P}_f(0, 1)$, the proposed AL-ABALQ method can also generate the time-dependent failure probability function $\hat{P}_f(0, t)$ for $t \in [0, 1]$ as a by-product. The statistical results are shown in Fig. 2, with comparison to the reference by MCS. It can be seen that the mean curve is close to the reference, and the mean \pm standard deviation (std dev) band remains narrow.

4.2. Example 2: a two-bar frame

The second numerical example involves a two-bar frame subjected to a time-varying stochastic load F(t) [45], as shown in Fig. 3. The two bars $(O_1O_2$ and $O_2O_3)$ have diameters d_1 and d_2 , respectively. Their yield strengths degrade over time, i.e., $s_1(t) = s_{1,0} \exp(-kt)$ and $s_2(t) = s_{2,0} \exp(-kt)$, where $s_{1,0}$ and $s_{2,0}$ are the initial yield strengths and k = 0.01. The distances O_1O_2 and O_1O_3 are denoted by l_1 and l_2 , respectively. Failure occurs when the axial stress in either bar exceeds its yield strength. The corresponding time-dependent performance function can be defined as:

$$g(\boldsymbol{X}, Y(t), t) = \min \begin{cases} \frac{\pi}{4} d_1^2 s_1(t) - \frac{l_1}{l_2} F(t), \\ \frac{\pi}{4} d_2^2 s_2(t) - \frac{\sqrt{l_1^2 + l_2^2}}{l_2} F(t) \end{cases} , \tag{36}$$

where $t \in [0, 15]$ year; $X = [d_1, d_2, s_{1,0}, s_{2,0}, l_1, l_2]$ is a set of six random variables, and Y(t) = F(t) is a stochastic process, as given in Table 3. In this example, n_t is set to be 50.

The results of several methods are presented in Table 4. The reference solution for the time-dependent failure probability $P_f(0,15)$ is taken as 8.13×10^{-3} (CoV = 0.35%), obtained using MCS with 50×10^7 samples. The proposed SL-ABALQ method achieves a comparable mean failure probability estimate with a significantly lower mean number of g-function evaluations (25.55) and a moderate CoV of 4.50%. In contrast, the PHI2 method requires 1224 g-function calls, but produces an inaccurate failure probability

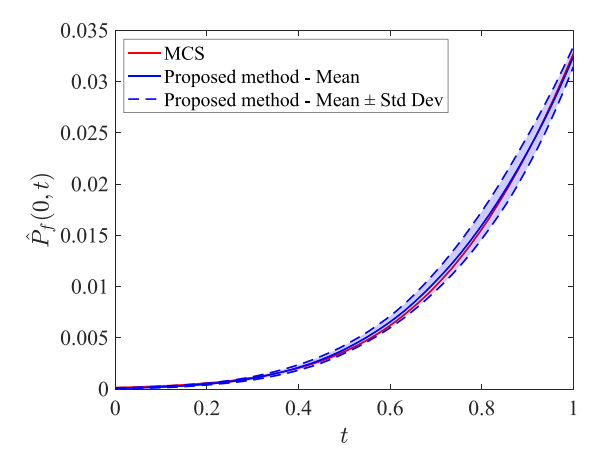


Fig. 2. Time-dependent failure probability function of Example 1.

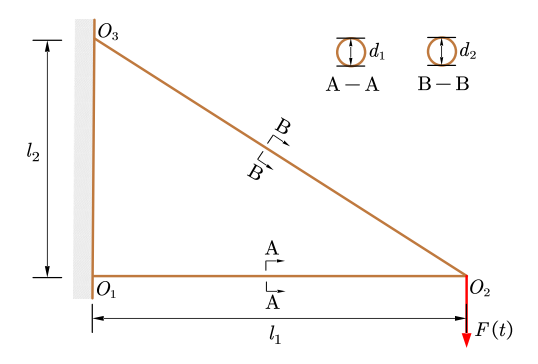


Fig. 3. A two-bar frame under a time-varying stochastic load.

Table 3Random variables and stochastic process of Example 2.

Symbol	Distribution	Mean	CoV	Auto-correlation function
d ₁ (m)	Uniform	0.10	0.025	-
d ₂ (m)	Uniform	0.12	0.025	_
s _{1.0} (Pa)	Lognormal	6×10^{8}	0.1	_
s _{2.0} (Pa)	Lognormal	6×10^{8}	0.1	-
l ₁ (m)	Uniform	0.4	0.025	_
l ₂ (m)	Uniform	0.3	0.025	_
F(t) (N)	Gaussian process	2×10^6	0.1	$\exp\left(-(t_2-t_1)^2/2\right)$

estimate of 1.53×10^{-2} . The SILK method failed to provide results due to an out-of-memory error before reaching its stopping criterion. Both the SL-GPR-AL and REAL methods also yield mean failure probability estimates close to the reference, with CoVs of 5.95% and 2.46%, respectively. However, they require more evaluations of the *g*-function on average than the proposed method, and the CoV of the number of *g*-function for REAL is notably high (40.87%).

Fig. 4 depicts the mean, mean \pm std dev of the time-dependent failure probability function $\hat{P}_f(0,t)$ for $t \in [0,15]$ from the proposed method, as well as the reference curve generated via MCS. It is shown that the mean curve accords well with the reference one, and the mean \pm std dev band is relatively narrow.

4.3. Example 3: a cantilever tube

In the third numerical example, we consider a cantilever tube subjected to two forces (F and P) and a time-varying torque (T(t)), as shown in Fig. 5. The tube has a length of L, and the hollow cross-section has outer radius r_o and inner radius r_i . The material's yield strength degrades over time according to $S(t) = S_0(1 - \gamma \log(1 + t))$, where S_0 is the initial yield strength and $\gamma = 0.01$. Failure is defined as the maximum von Mises stress exceeding the yield strength. The associated time-dependent performance function is

Table 4Time-dependent failure probability results of Example 2.

Method	$N_{ m call}$		$\hat{P}_f(0,15)$	
	Mean	CoV	Mean	CoV
MCS	50 × 10 ⁷	_	8.13×10^{-3}	0.35%
PHI2	1224	_	1.53×10^{-2}	_
SILK	-	-	_	-
REAL	46.35	40.87%	8.04×10^{-3}	2.46%
SL-GPR-AL	31.50	9.30%	8.08×10^{-3}	5.95%
Proposed SL-ABALQ	25.55	12.34%	8.14×10^{-3}	4.50%

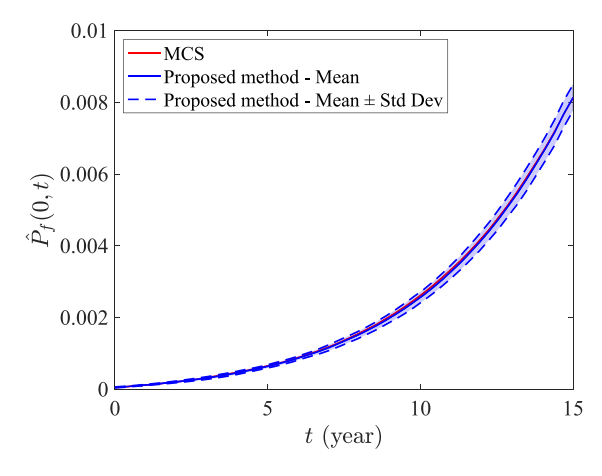


Fig. 4. Time-dependent failure probability function of Example 2.

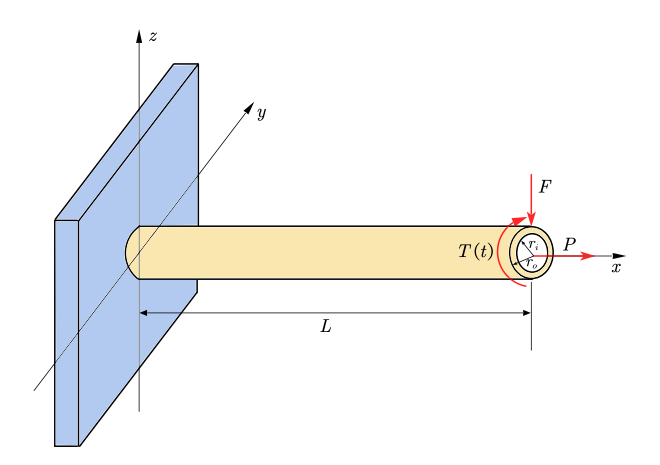


Fig. 5. A cantilever tube under two forces and one torque.

given by:

$$g(X,Y(t),t) = S(t) - \sqrt{\left(\frac{P}{\pi(r_o^2 - r_i^2)} + \frac{FLr_o}{\frac{\pi}{4}(r_o^4 - r_i^4)}\right)^2 + 3\left(\frac{T(t)r_o}{\frac{\pi}{2}(r_o^4 - r_i^4)}\right)^2},$$
(37)

where $t \in [0, 5]$ year; $X = [S_0, r_i, r_o, L, F, P]$ is a vector of six random variables, and Y(t) = T(t) is a stochastic process, as given in Table 5. In this example, we set $n_t = 20$.

Table 6 compares the performance of several methods. The reference value for the time-dependent failure probability $P_f(0,5)$ is 1.18×10^{-2} (with a small CoV of 0.41%), which is given by MCS with $20 \times 5 \times 10^6$ samples. The PHI2 method requires 3360 evaluations of the performance function and produces a failure probability estimate of 2.29×10^{-2} , which deviates significantly from the reference value. The results of SILK are unavailable, as it ran out of memory before reaching its stopping criterion. Among the remaining methods, the proposed SL-ABALQ achieves the lowest average number of g-function evaluations, with a mean of only

Table 5Random variables and stochastic process of Example 3.

Symbol	Distribution	Mean	CoV	Auto-correlation function
S_0 (MPa)	Lognormal	320	0.10	-
r_i (mm)	Uniform	10	0.05	-
r_o (mm)	Uniform	20	0.05	_
L (mm)	Uniform	120	0.05	-
F (kN)	Lognormal	5	0.05	_
P (kN)	Lognormal	10	0.10	-
T(t) (N m)	Gaussian process	1000	0.15	$\exp\left(-(t_2-t_1)^2/5\right)$

Table 6Time-dependent failure probability results of Example 3.

Method	$N_{ m call}$		$\hat{P}_f(0,5)$		
	Mean	CoV	Mean	CoV	
MCS	$20 \times 5 \times 10^{6}$	_	1.18×10^{-2}	0.41%	
PHI2	3360	_	2.29×10^{-2}	_	
SILK	-	-	_	_	
REAL	53.70	13.02%	1.21×10^{-2}	2.22%	
SL-GPR-AL	37.25	15.16%	1.16×10^{-2}	4.16%	
Proposed SL-ABALQ	20.05	7.84%	1.16×10^{-2}	3.90%	

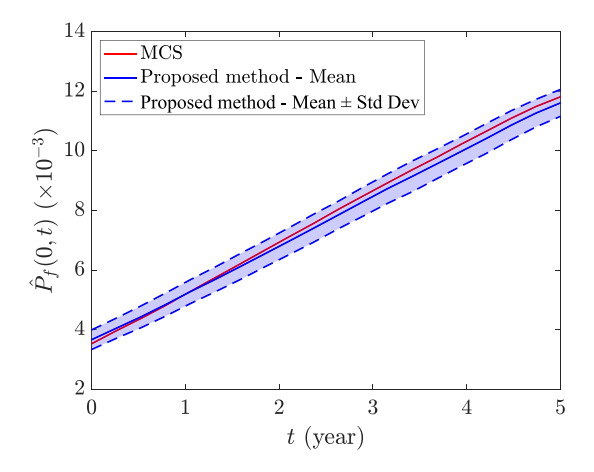


Fig. 6. Time-dependent failure probability function of Example 3.

20.05 and a CoV of 7.84%. Moreover, it provides a mean failure probability estimate that closely matches the reference, along with a low CoV of 3.90%.

Fig. 6 shows the statistical results of the time-dependent failure probability function $\hat{P}_f(0,t)$ for $t \in [0,5]$, along with the reference produced by MCS. The mean curve is in good agreement with the reference, while the mean \pm std dev band is suitably narrow.

4.4. Example 4: a space truss

The fourth example consists of a 120-bar space truss structure under thirteen vertical loads (which has been studied in, e.g., [32,40]), as sketched in Fig. 7. The finite-element model of this structure is created using the software called OpenSees (https://opensees.berkeley.edu/), comprising 120 truss elements and 49 nodes. Each bar has a cross-sectional area A, and is made of a material with Young's modulus E. Twelve static loads P_1, P_2, \ldots, P_{12} are applied at nodes 1–12, while a time-varying load $P_0(t)$ is imposed at node 0. The time-dependent performance function is defined as:

$$g(X, Y(t)) = \Delta - V_0(A, E, P_0(t), P_1, P_2, \dots, P_{12}),$$
(38)

where $t \in [0, 50]$ year; V_0 is the vertical displacement of node 0; Δ is the tolerance, which is specified as 100 mm; $X = [A, E, P_1, P_2, \dots, P_{12}]$ is a vector of fourteen random variables, $Y(t) = P_0(t)$ is a stochastic process, as given in Table 7. In this example, $n_t = 50$ is used.

Table 8 reports the results obtained by various methods for estimating the time-dependent failure probability $P_f(0,50)$. The reference failure probability is taken as 2.85×10^{-2} (CoV = 0.82%), generated by MCS with $50 \times 5 \times 10^{5}$ model evaluations. The PHI2 method produces an inaccurate failure probability estimate of 3.20×10^{-2} , while requiring 1664 evaluations of the performance

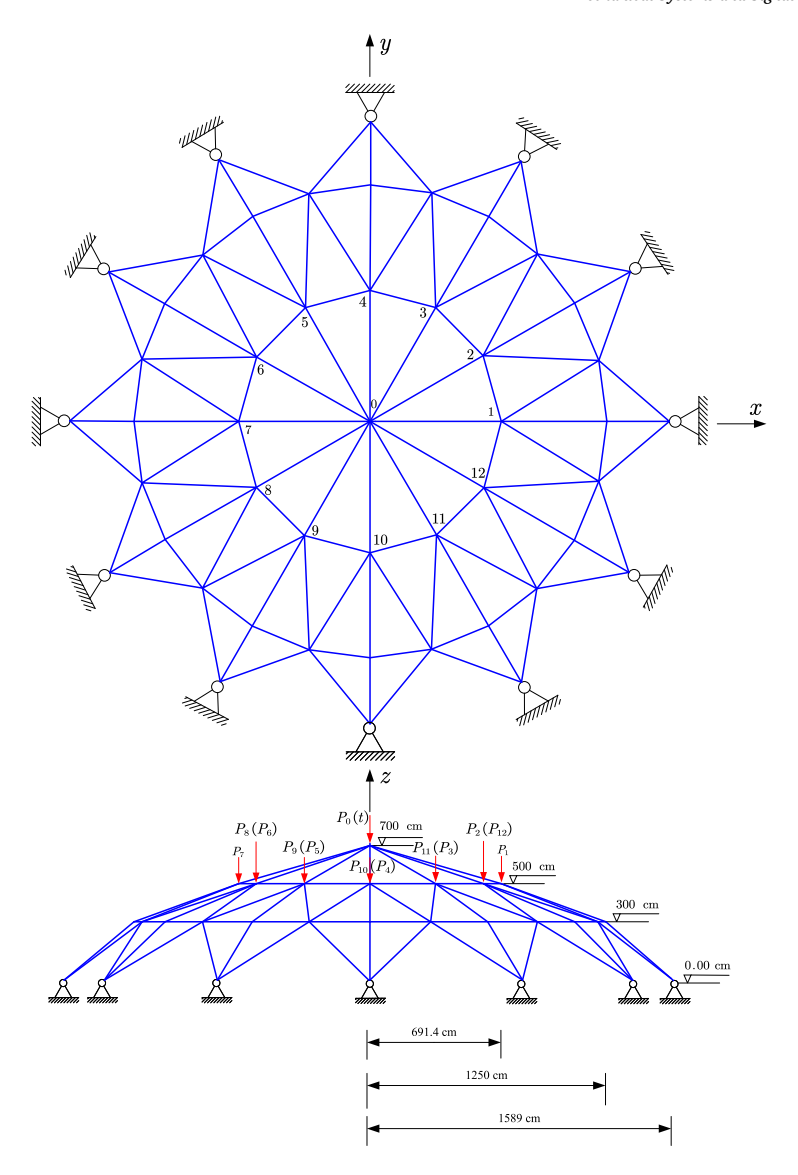


Fig. 7. A 120-bar space truss subject to thirteen vertical loads [40].

Table 7
Random variables and stochastic process of Example 4.

Symbol	Distribution	Mean	CoV	Auto-correlation function
A (mm ²)	(Truncated) Normal	2000	0.10	_
E (GPa)	(Truncated) Normal	200	0.10	_
P_1, P_2, \dots, P_{12} (kN)	Lognormal	100	0.15	_
$P_0(t)$ (kN)	Lognormal process	1000	0.15	$\exp\left(-(t_2 - t_1)^2 / 50\right)$

Note: The auto-correlation coefficient function for $P_0(t)$ is defined for the underlying Gaussian process.

function. The results of SILK and REAL are missing as both methods ran out of memory before reaching their stopping criteria. At the cost of an average of 44.40 model calls, SL-GPR-AL gives a failure probability mean (2.89×10^{-2}) that is close to the reference with a small CoV of 1.73%. In contrast, the proposed SL-ABALQ method only requires 35.25 model evaluations on average, while still delivering fairly good results.

Fig. 8 shows the statistical results for the time-dependent failure probability function $\hat{P}_f(0,t)$ for $t \in [0,50]$ alongside the reference curve generated by MCS. It can be seen that the mean \pm std dev band is narrow and the mean curve is close to the reference curve.

 Table 8

 Time-dependent failure probability results of Example 4.

Method	$N_{ m call}$		$\hat{P}_f(0,50)$		
	Mean	CoV	Mean	CoV	
MCS	$50 \times 5 \times 10^{5}$	_	2.85×10^{-2}	0.82%	
PHI2	1664	_	3.20×10^{-2}	-	
SILK	-	_	_	_	
REAL	-	_	_	_	
SL-GPR-AL	44.40	9.73%	2.89×10^{-2}	1.73%	
Proposed SL-ABALQ	35.25	10.57%	2.88×10^{-2}	3.33%	

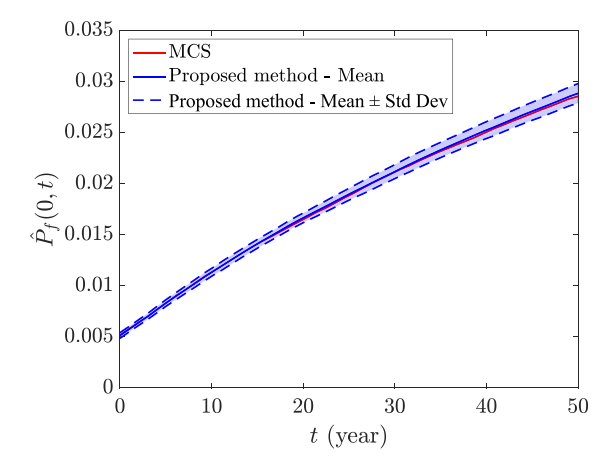


Fig. 8. Time-dependent failure probability function of Example 4.

Table 9Random variables and stochastic process of Example 5.

Symbol	Distribution	Mean	CoV	Auto-correlation function
E_0 (GPa)	Lognormal	210	0.10	_
$f_{v,0}$ (MPa)	Lognormal	300	0.10	_
b	Uniform	0.02	0.02	_
Q_D (kN/m)	Lognormal	20	0.10	-
$Q_{L,1}, \dots, Q_{L,4} \text{ (kN/m)}$	Lognormal	10	0.10	-
F(t) (kN)	Gaussian process	$200(1+0.05\log(1+t))$	0.15	$\exp\left(- t_2-t_1 /25\right)$

4.5. Example 5: a steel frame

The final example involves a three-bay, four-story steel frame structure, as shown in Fig. 9(a). As in Example 4, this structure is also modeled using the software OpenSees. The model comprises 12 beam and 16 column members, each represented as a nonlinear beam—column element. The P- Δ effect is explicitly accounted for in all columns. The cross-section is I-shaped, as shown in Fig. 9(b), with dimensions d=0.5 m, $b_f=0.3$ m, and $t_w=t_f=0.02$ m. The constitutive law of the steel is represented by a bilinear model, as depicted in Fig. 9(c). The modulus of elasticity and yield strength degrade over time according to $E(t)=E_0(1-\gamma\log(1+t))$ and $f_y(t)=f_{y,0}(1-\gamma\log(1+t))$, where E_0 and $f_{y,0}$ are the initial modulus of elasticity and yield strength respectively, and $\gamma=0.05$. The strain-hardening ratio is denoted by b. As shown in Fig. 9(a), each floor is subjected to a uniformly distributed dead load Q_D and a live load $Q_{L,i}$. In addition, four time-dependent lateral loads are applied, i.e., $\frac{1}{4}F(t)$, $\frac{1}{2}F(t)$, $\frac{3}{4}F(t)$, and F(t). The time-dependent performance function is defined as:

$$g(X, Y(t), t) = \Delta - U_4(E_0, f_{y,0}, b, Q_D, D_{L,1}, D_{L,2}, D_{L,3}, D_{L,4}, F(t), t),$$
(39)

where $t \in [0, 2.5]$ year; U_4 denotes the lateral displacement of the fourth floor (specifically, at the left-top node); Δ is the threshold, which is set to 0.024 m; $X = [E_0, f_{y,0}, b, Q_D, D_{L,1}, D_{L,2}, D_{L,3}, D_{L,4}]$ is a vector of eight independent random variables, Y(t) = F(t) is a stochastic process, as detailed in Table 9. In this example, n_t is set to 25.

The results of several methods are summarized in Table 10. The reference value of the time-dependent failure probability $P_f(0, 2.5)$, obtained from MCS with 25×10^5 simulations, is 1.89×10^{-2} with a CoV of 2.28%. The PHI2 method gives an inaccurate estimate, i.e., 2.90×10^{-2} , with 770 model evaluations. The results of both SILK and REAL are unavailable as in some trials they ran out of memory before reaching their respective stopping criteria. Compared with SL-GPR-AL, the proposed SL-ABALQ method demonstrates better overall performance: (1) it requires slightly fewer g-function calls on average (15.50 vs. 16.55), with similar

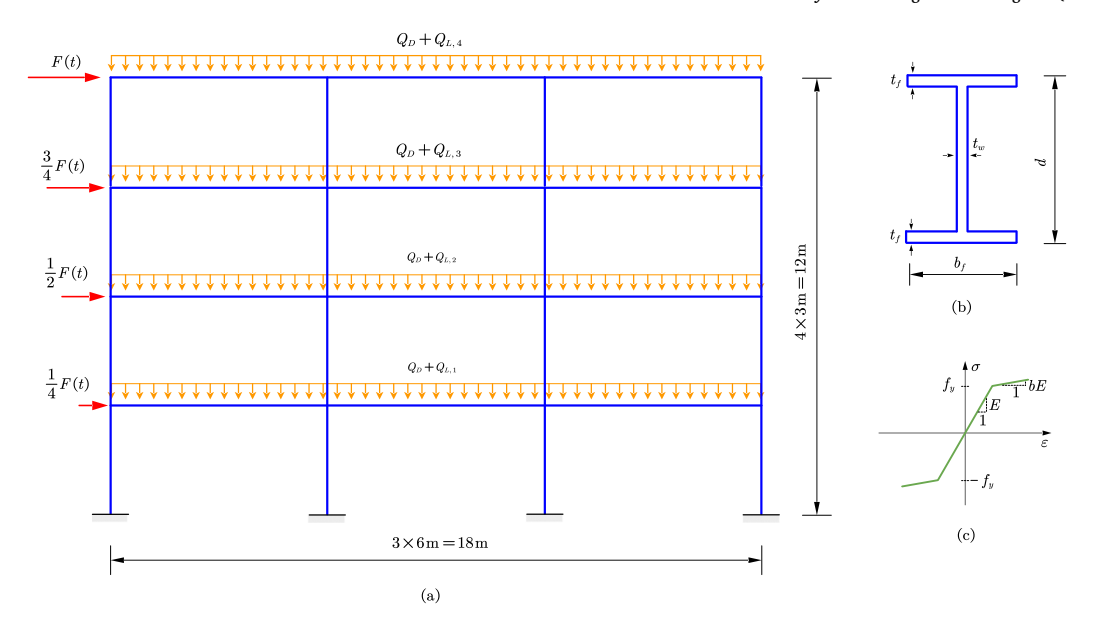


Fig. 9. A three-bay, four-story steel frame structure subjected to vertical and lateral loads.

Table 10
Time-dependent failure probability results of Example 5.

Method	$N_{ m call}$		$\hat{P}_f(0, 2.5)$	
	Mean	CoV	Mean	CoV
MCS	25 × 10 ⁵	_	1.89×10^{-2}	2.28%
PHI2	770	_	2.90×10^{-2}	_
SILK	_	_	_	_
REAL	-	_	_	-
SL-GPR-AL	16.55	9.29%	1.85×10^{-2}	5.12%
Proposed SL-ABALQ	15.50	9.24%	1.87×10^{-2}	4.54%

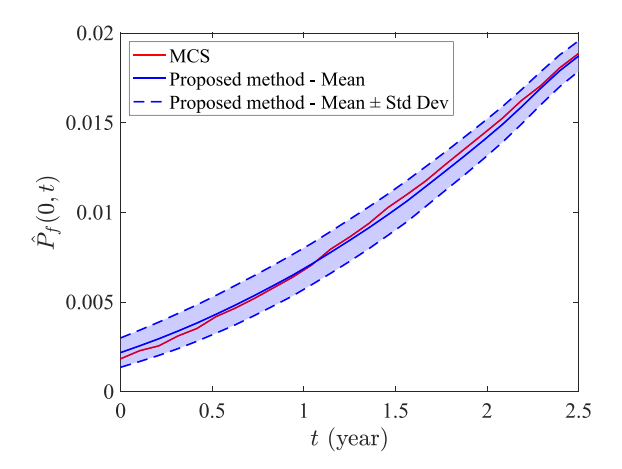


Fig. 10. Time-dependent failure probability function of Example 5.

CoVs (9.24% vs. 9.29%); and (2) it yields a slightly smaller CoV for the failure probabilities (4.54% vs. 5.12%), while the mean values of both methods remain very close to the reference.

Fig. 10 shows the statistical results of the time-dependent failure probability function $\hat{P}_f(0,t)$ for $t \in [0,2.5]$ obtained by the proposed method, together with the reference solution from MCS. It can be seen that the mean curve is close to the reference, accompanied by a narrow mean \pm std dev band.

5. Summary and conclusions

This paper presents a novel method for computationally expensive time-dependent structural reliability analysis, termed 'single-loop approximate Bayesian active learning quadrature' (SL-ABALQ). In this method, the integral of the time-dependent failure probability is addressed from a Bayesian active learning perspective in a single-loop format. By virtue of the Bayesian nature of Gaussian process regression (GPR), an approximate Bayesian inference scheme is developed to avoid the potential intractability of exact Bayesian inference. This approach yields both an estimator for the time-dependent failure probability and an associated measure of uncertainty. Building on these results, we propose a novel stopping criterion that determines when the iterative process should terminate, thereby avoiding both premature convergence and unnecessary continuation. In addition, two new learning functions are presented to guide the selection of the next best time instant and the sample point of random variables and stochastic processes (at the selected time instant) at which to evaluate the performance function if the stopping criterion is not reached. The performance of the proposed SL-ABALQ method is demonstrated through five numerical examples against several existing methods. It is shown that our method can reduce the number of performance function evaluations without sacrificing accuracy. The method is designed for the general time-dependent reliability problems, where the performance function is a function of input random variables, stochastic processes and the time parameter. Of course, it is equally applicable to some other special cases. Moreover, AL-ABALQ can provide the evolution of failure probability over the time interval at no additional computational cost.

Future research could explore the following aspects. First, efficient stochastic simulation techniques could be employed to replace the plain MCS, particularly when the time-dependent failure probability over a given interval is very small. This is also relevant in cases where the quantity of interest is an accurate time-dependent failure probability function, as the failure probability is typically low at the beginning of the time interval. Second, multi-point selection strategies can be developed to facilitate the parallel distributed processing, thus further enhancing the computational efficiency. Third, although the proposed method can alleviate the curse of dimensionality to some extent — since each input stochastic process is treated as a single dimension — dimension-reduction techniques may still be beneficial when the total dimensionality (i.e., $d_1 + d_2 + 1$) is high.

CRediT authorship contribution statement

Chao Dang: Writing – original draft, Visualization, Validation, Methodology, Investigation, Conceptualization. Pei-Pei Li: Writing – review & editing, Validation, Funding acquisition. Marcos A. Valdebenito: Writing – review & editing, Validation, Supervision, Project administration. Matthias G.R. Faes: Writing – review & editing, Validation, Supervision, Resources, Project administration, Funding acquisition.

Declaration of competing interest

The authors declare that they have no known competing financial interests or personal relationships that could have appeared to influence the work reported in this paper.

Acknowledgments

Chao Dang is grateful for the financial support of the German Research Foundation (DFG) (Grant number 530326817). Pei-Pei Li and Matthias Faes acknowledge the Alexander von Humboldt Foundation for the postdoctoral grant and the Henriette Herz Scouting program, respectively.

Data availability

No data was used for the research described in the article.

References

- [1] S.O. Rice, Mathematical analysis of random noise, Bell Syst. Tech. J. 23 (3) (1944) 282-332, http://dx.doi.org/10.1002/j.1538-7305.1944.tb00874.x.
- [2] H. Cramér, M.R. Leadbetter, Stationary and Related Stochastic Processes: Sample Function Properties and Their Applications, Courier Corporation, 2013.
- [3] A. Firouzi, W. Yang, C.-Q. Li, Efficient solution for calculation of upcrossing rate of nonstationary Gaussian process, J. Eng. Mech. 144 (4) (2018) 04018015, http://dx.doi.org/10.1061/(ASCE)EM.1943-7889.0001420.
- [4] C.-Q. Li, A. Firouzi, W. Yang, Closed-form solution to first passage probability for nonstationary lognormal processes, J. Eng. Mech. 142 (12) (2016) 04016103, http://dx.doi.org/10.1061/(ASCE)EM.1943-7889.0001160.
- [5] C. Andrieu-Renaud, B. Sudret, M. Lemaire, The PHI2 method: a way to compute time-variant reliability, Reliab. Eng. Syst. Saf. 84 (1) (2004) 75–86, http://dx.doi.org/10.1016/j.ress.2003.10.005.
- [6] B. Sudret, Analytical derivation of the outcrossing rate in time-variant reliability problems, Struct. Infrastruct. Eng. 4 (5) (2008) 353–362, http://dx.doi.org/10.1080/15732470701270058.
- [7] X.-Y. Zhang, Z.-H. Lu, S.-Y. Wu, Y.-G. Zhao, An efficient method for time-variant reliability including finite element analysis, Reliab. Eng. Syst. Saf. 210 (2021) 107534, http://dx.doi.org/10.1016/j.ress.2021.107534.
- [8] W. Chen, B. Ni, W. Tian, C. Jiang, The first-order time-variant reliability expansion method, Struct. Saf. 109 (2024) 102484, http://dx.doi.org/10.1016/j.strusafe.2024.102484.
- [9] W. Du, Y. Luo, Y. Wang, Time-variant reliability analysis using the parallel subset simulation, Reliab. Eng. Syst. Saf. 182 (2019) 250–257, http://dx.doi.org/10.1016/j.ress.2018.10.016.

- [10] H.-S. Li, T. Wang, J.-Y. Yuan, H. Zhang, A sampling-based method for high-dimensional time-variant reliability analysis, Mech. Syst. Signal Process. 126 (2019) 505–520, http://dx.doi.org/10.1016/j.ymssp.2019.02.050.
- [11] D.Y. Yang, J.-G. Teng, D.M. Frangopol, Cross-entropy-based adaptive importance sampling for time-dependent reliability analysis of deteriorating structures, Struct. Saf. 66 (2017) 38–50, http://dx.doi.org/10.1016/j.strusafe.2016.12.006.
- [12] J. Wang, R. Cao, Z. Sun, Importance sampling for time-variant reliability analysis, IEEE Access 9 (2021) 20933–20941, http://dx.doi.org/10.1109/ACCESS. 2021 3054470
- [13] X. Yuan, S. Liu, M. Faes, M.A. Valdebenito, M. Beer, An efficient importance sampling approach for reliability analysis of time-variant structures subject to time-dependent stochastic load, Mech. Syst. Signal Process. 159 (2021) 107699, http://dx.doi.org/10.1016/j.ymssp.2021.107699.
- [14] X. Yuan, Y. Shu, Y. Qian, Y. Dong, Adaptive importance sampling approach for structural time-variant reliability analysis, Struct. Saf. 111 (2024) 102500, http://dx.doi.org/10.1016/j.strusafe.2024.102500.
- [15] X. Yuan, W. Zheng, C. Zhao, M.A. Valdebenito, M.G. Faes, Y. Dong, Line sampling for time-variant failure probability estimation using an adaptive combination approach, Reliab. Eng. Syst. Saf. 243 (2024) 109885, http://dx.doi.org/10.1016/j.ress.2023.109885.
- [16] D. Zhang, X. Han, C. Jiang, J. Liu, Q. Li, Time-dependent reliability analysis through response surface method, J. Mech. Des. 139 (4) (2017) 041404, http://dx.doi.org/10.1115/1.4035860.
- [17] L. Hawchar, C.-P. El Soueidy, F. Schoefs, Principal component analysis and polynomial chaos expansion for time-variant reliability problems, Reliab. Eng. Syst. Saf. 167 (2017) 406–416, http://dx.doi.org/10.1016/j.ress.2017.06.024.
- [18] W. Zheng, X. Yuan, X. Bao, Y. Dong, Adaptive support vector machine for time-variant failure probability function estimation, Reliab. Eng. Syst. Saf. 253 (2025) 110510, http://dx.doi.org/10.1016/j.ress.2024.110510.
- [19] Z. Wang, P. Wang, A nested extreme response surface approach for time-dependent reliability-based design optimization, J. Mech. Des. 134 (12) (2012) 121007, http://dx.doi.org/10.1115/1.4007931.
- [20] Z. Hu, X. Du, Mixed efficient global optimization for time-dependent reliability analysis, J. Mech. Des. 137 (5) (2015) 051401, http://dx.doi.org/10.1115/ 1.4029520.
- [21] J. Wu, Z. Jiang, H. Song, L. Wan, F. Huang, Parallel efficient global optimization method: A novel approach for time-dependent reliability analysis and applications, Expert Syst. Appl. 184 (2021) 115494, http://dx.doi.org/10.1016/j.eswa.2021.115494.
- [22] C. Ling, Z. Lu, X. Zhu, Efficient methods by active learning Kriging coupled with variance reduction based sampling methods for time-dependent failure probability, Reliab. Eng. Syst. Saf. 188 (2019) 23–35, http://dx.doi.org/10.1016/j.ress.2019.03.004.
- [23] H. Li, Z. Lu, K. Feng, A double-loop Kriging model algorithm combined with importance sampling for time-dependent reliability analysis, Eng. Comput. 40 (3) (2024) 1539–1558, http://dx.doi.org/10.1007/s00366-023-01879-8.
- [24] Z. Hu, S. Mahadevan, A single-loop Kriging surrogate modeling for time-dependent reliability analysis, J. Mech. Des. 138 (6) (2016) 061406, http://dx.doi.org/10.1115/1.4033428.
- [25] W. Yun, Z. Lu, X. Jiang, L.F. Zhao, Maximum probable life time analysis under the required time-dependent failure probability constraint and its meta-model estimation, Struct. Multidiscip. Optim. 55 (2017) 1439–1451, http://dx.doi.org/10.1007/s00158-016-1594-z.
- [26] C. Jiang, D. Wang, H. Qiu, L. Gao, L. Chen, Z. Yang, An active failure-pursuing Kriging modeling method for time-dependent reliability analysis, Mech. Syst. Signal Process. 129 (2019) 112–129, http://dx.doi.org/10.1016/j.ymssp.2019.04.034.
- [27] C. Jiang, H. Qiu, L. Gao, D. Wang, Z. Yang, L. Chen, Real-time estimation error-guided active learning Kriging method for time-dependent reliability analysis, Appl. Math. Model. 77 (2020) 82–98, http://dx.doi.org/10.1016/j.apm.2019.06.035.
- [28] Y. Hu, Z. Lu, N. Wei, C. Zhou, A single-loop Kriging surrogate model method by considering the first failure instant for time-dependent reliability analysis and safety lifetime analysis, Mech. Syst. Signal Process. 145 (2020) 106963, http://dx.doi.org/10.1016/j.ymssp.2020.106963.
- [29] D. Wang, H. Qiu, L. Gao, C. Jiang, A single-loop Kriging coupled with subset simulation for time-dependent reliability analysis, Reliab. Eng. Syst. Saf. 216 (2021) 107931, http://dx.doi.org/10.1016/j.ress.2021.107931.
- [30] Z. Song, H. Zhang, L. Zhang, Z. Liu, P. Zhu, An estimation variance reduction-guided adaptive Kriging method for efficient time-variant structural reliability analysis, Mech. Syst. Signal Process. 178 (2022) 109322, http://dx.doi.org/10.1016/j.ymssp.2022.109322.
- [31] D. Wang, H. Qiu, L. Gao, C. Jiang, A subdomain uncertainty-guided Kriging method with optimized feasibility metric for time-dependent reliability analysis, Reliab. Eng. Syst. Saf. 243 (2024) 109839. http://dx.doi.org/10.1016/j.ress.2023.109839.
- [32] C. Dang, M.A. Valdebenito, M.G. Faes, Towards a single-loop Gaussian process regression based-active learning method for time-dependent reliability analysis, Mech. Syst. Signal Process. 226 (2025) 112294, http://dx.doi.org/10.1016/j.ymssp.2024.112294.
- [33] Z. Hu, C. Dang, D. Wang, M. Beer, L. Wang, Error-informed parallel adaptive Kriging method for time-dependent reliability analysis, Reliab. Eng. Syst. Saf. (2025) 111194. http://dx.doi.org/10.1016/j.ress.2025.111194.
- [34] C. Dang, P. Wei, J. Song, M. Beer, Estimation of failure probability function under imprecise probabilities by active learning-augmented probabilistic integration, ASCE-ASME J. Risk Uncertain. Eng. Syst., Part A: Civ. Eng. 7 (4) (2021) 04021054, http://dx.doi.org/10.1061/AJRUA6.0001179.
- [35] C. Dang, M. Beer, Semi-Bayesian active learning quadrature for estimating extremely low failure probabilities, Reliab. Eng. Syst. Saf. 246 (2024) 110052, http://dx.doi.org/10.1016/j.ress.2024.110052.
- [36] C. Dang, M.G. Faes, M.A. Valdebenito, P. Wei, M. Beer, Partially Bayesian active learning cubature for structural reliability analysis with extremely small failure probabilities, Comput. Methods Appl. Mech. Engrg. 422 (2024) 116828, http://dx.doi.org/10.1016/j.cma.2024.116828.
- [37] C. Dang, A. Cicirello, M.A. Valdebenito, M.G. Faes, P. Wei, M. Beer, Structural reliability analysis with extremely small failure probabilities: A quasi-Bayesian active learning method, Probabilistic Eng. Mech. 76 (2024) 103613, http://dx.doi.org/10.1016/j.probengmech.2024.103613.
- [38] C. Dang, T. Zhou, M.A. Valdebenito, M.G. Faes, Yet another Bayesian active learning reliability analysis method, Struct. Saf. 112 (2025) 102539, http://dx.doi.org/10.1016/j.strusafe.2024.102539.
- [39] Z. Hu, D. Wang, C. Dang, M. Beer, L. Wang, Uncertainty-aware adaptive Bayesian inference method for structural time-dependent reliability analysis, Reliab. Eng. Syst. Saf. (2025) Under Review.
- [40] C. Dang, M.A. Valdebenito, M.G. Faes, Time-dependent reliability analysis by a single-loop Bayesian active learning method using Gaussian process regression, Comput. Methods Appl. Mech. Engrg. 444 (2025) 118092, http://dx.doi.org/10.1016/j.cma.2025.118092.
- [41] K.-K. Phoon, S. Huang, S.T. Quek, Simulation of second-order processes using Karhunen-Loeve expansion, Comput. Struct. 80 (12) (2002) 1049–1060, http://dx.doi.org/10.1016/S0045-7949(02)00064-0.
- [42] C.K. Williams, C.E. Rasmussen, Gaussian Processes for Machine Learning, vol. 2, (3) MIT press Cambridge, MA, 2006.
- [43] C. Dang, P. Wei, M.G. Faes, M.A. Valdebenito, M. Beer, Parallel adaptive Bayesian quadrature for rare event estimation, Reliab. Eng. Syst. Saf. 225 (2022) 108621, http://dx.doi.org/10.1016/j.ress.2022.108621.
- [44] C. Dang, M.A. Valdebenito, M.G. Faes, P. Wei, M. Beer, Structural reliability analysis: A Bayesian perspective, Struct. Saf. 99 (2022) 102259, http://dx.doi.org/10.1016/j.strusafe.2022.102259.
- [45] Z. Hu, X. Du, Reliability-based design optimization under stationary stochastic process loads, Eng. Optim. 48 (8) (2016) 1296–1312, http://dx.doi.org/10.1080/0305215X.2015.1100956.